Research Article

Aerodynamic Analysis of NACA 4412 Airfoil with CFD for Small Scale Wind Turbine Design

Mehmet Bakırcı [1] **, Refik Polat** [2] **and Mehmet Tayyip Özdemir** [2,*]

[1] Karabük University, Faculty of Engineering, Department of Mechanical Engineering, 78050, Karabük/Turkey
[2] Selçuk University, Faculty of Technology, Department of Mechanical Engineering, 42100, Konya/Turkey
* Correspondence: tayyipozdemir@karabuk.edu.tr

Abstract: With the increasing population in our country, the need for energy is increasing. Therefore, interest in renewable and clean energy matters in recent years. The wind turbine obtains electricity from wind energy, which is a renewable energy source. One of the elements affecting the yield of wind turbines is aerodynamic properties of airfoils. In this study, CFD analysis of NACA 4412 Airfoil which can be used in small scale wind turbine design was performed. Compared to literature, there were differences in the number of Reynolds due to the size difference of airfoil. Therefore, small deviations occurred in the aerodynamic properties of airfoil. Additionally, in this study, it was concluded that 15° angle of attack is the stall angle for NACA 4412 airfoil. It has been observed that as the angle of attack increases, the Reynolds number decreases and the drag coefficient value increases. In other words, it has been concluded that aerodynamic performance is negatively affected by increasing the drag coefficient value. As a result of the analyses, results consistent with the experimental studies were obtained.

Keywords: airfoil; aerodynamic; CFD

Küçük Ölçekli Rüzgâr Türbini Tasarımı için NACA 4412 Kanat Profilinin HAD ile Aerodinamik Analizi

Öz: Ülkemizde artan nüfusla birlikte enerjiye olan ihtiyaç da artmaktadır. Bundan dolayı yenilenebilir ve temiz enerjiye olan ilgi son yıllarda önem arz etmektedir. Rüzgâr türbini ise yenilenebilir enerji kaynağı olan rüzgâr enerjisinden elektrik elde etmektedir. Rüzgâr türbinlerinin verimini etkileyen unsurlardan birisi ise airfoillerin aerodinamik özellikleridir. Bu çalışmada küçük ölçekli rüzgâr türbin tasarımında kullanılabilecek olan NACA 4412 airfoilinin HAD analizi yapılmıştır. Literatürle kıyaslandığında airfoilin boyut farkından dolayı Reynolds sayısında farklılıklar görülmüştür. Bundan dolayı, airfoilin aerodinamik özelliklerinde küçük sapmalar meydana gelmiştir. Ayrıca bu çalışmada 15° hücum açısının NACA 4412 airfoili için stall açısı olduğu sonucuna ulaşılmıştır. Hücum açısı arttıkça Reynolds sayısının düştüğü ve sürükleme katsayı değerinin arttığı gözlemlenmiştir. Yani sürükleme katsayı değerinin artmasıyla aerodinamik performansın olumsuz etkilenmesi sonucuna ulaşılmıştır. Yapılan analizler neticesinde deneysel olarak yapılan çalışmalarla örtüşen sonuçlar elde edilmiştir.

Anahtar Kelimeler: airfoil; aerodinamik, HAD

1. Introduction

With the rapid population growth in our country, obtaining energy from wind has been developing significantly in recent years. The fact that wind energy is renewable, clean and endless is one of the important reasons for this development. However, the competition between industrially developed countries has also increased the importance of wind energy. In this context, further development of wind turbines is important. Studies continue all over the world to increase the durability of wind turbines, increase their efficiency and make the most appropriate design for different wind speeds [1]–[3]. One of the most important elements affecting the efficiency of wind turbines is blade aerodynamics. The aerodynamic design of wing section (airfoil) geometries affects the performance of the entire wing and therefore the total efficiency of the wind turbine [4]. Airfoil design for wind turbine blades is critical in wind turbine development. Studies have shown that optimum airfoil selection reduces the cost of energy production. Airfoil design is done to achieve the optimum situation between strength requirements, manufacturing difficulties and aerodynamic performance. For example; Achieving a high lift/drag ratio and insensitivity to roughness is good for aerodynamic performance. The aim of this study is to produce airfoil with higher lift force, which can be used in later studies, especially in wind turbine blades. One of the most used airfoil geometries in wind turbine blades is the NACA series developed by the National Advisory Committee for Aeronautics (NACA). This series has four-, five- and six-digit variants. In this study, NACA 4412 section, which is from the four-digit series, was used. Bakırcı carried out horizontal axis wind turbine optimization in his doctoral study. He examined the compatibility of the results obtained with the BEM theorem, CFD (computational fluid dyna-mics) simulation and experimental studies. He calculated the design and tip speed ratios of the turbine he designed [5]. Kumar simulated and compared the aerodynamic performances of different airfoil types, NACA4412 and NREL S 809 airfoils, with the CFD method. As a result, he emphasized that the aerodynamic performance of the NACA series is better than the NREL series [6]. In their study, Kogaki et al. examined the vortex generators that affect airfoil performance in wind turbines. As a result of the CFD method and their studies in the wind tunnel, they observed that vortex generators with airfoil geometry are more efficient than rectangular cross-sections in small scale wind turbines [7]. Suzuki et al. [8] have shown through analytical and numerical analysis that the laminar drag force decreases for the new airfoil obtained by stretching the leading edge of the NACA 63012 airfoil geometry towards the bottom surface side. Hartwanger [9] performed the NREL S 809 airfoil CFD analysis in two dimensions using X-FOIL and Ansys CFX computer packages. He made the flow analysis so that the first part of the flow on the airfoil is laminar and the other part is turbulent. It has been shown that the values obtained with this model for pre-stall flow are fully compatible with the experimental results. Sarada, Shankar and Rudresh [10] made 2D (two-dimensional) and 3D (three-dimensional) CFD analysis of the NACA 64-618 airfoil geometry with the Ansys Fluent computer package program. They used the k-epsilon model in this study. With this turbulence model, in the stall situation, they could not obtain values close to the experimental data in 2D, but they could obtain them in 3D. When the studies in the literature are generally examined, airfoil has the highest lift force at a certain angle of at-tack. However, when the angle of attack increases further, it enters a stall state. In this case, the drag force increases [11], [12].

In this study, the aerodynamic analysis of the standard airfoil NACA 4412 was made with the standard k-epsilon turbulence model in the CFD computer package program and the results obtained were compared with the results of the originals obtained under the same conditions. In this study, it is aimed to determine the optimum speed and optimum angle of attack required for NACA 4412 used in wind turbine design to achieve higher lift force. This study aims to contribute to new studies.

2. Experimental

Standard NACA 4412 blade geometry was obtained from the literature [13], [14]. The obtained airfoil aerodynamic properties were analyzed by CFD.

2.1. Airfoil Aerodynamics

Airfoils are 2D sections of objects such as airplane wings, propellers, and wind turbine blades moving in a fluid. Airfoils moving through the fluid produce an aerodynamic force.

The component of this force perpendicular to the direction of motion is called lift. The component parallel to the direction of motion is called drag. Subsonic flight airfoils have a characteristic shape with a rounded leading edge followed by a sharp trailing edge, often asymmetrically cambered. Lift on an airfoil is primarily the result of its angle of attack and shape. When oriented at a proper angle, the airfoil deflects oncoming air, creating a force on the wing in the direction opposite to the deflection. As seen in Figure 1, most airfoil shapes require a positive angle of attack to create lift, but domed airfoils can create lift at zero angle of attack [15].
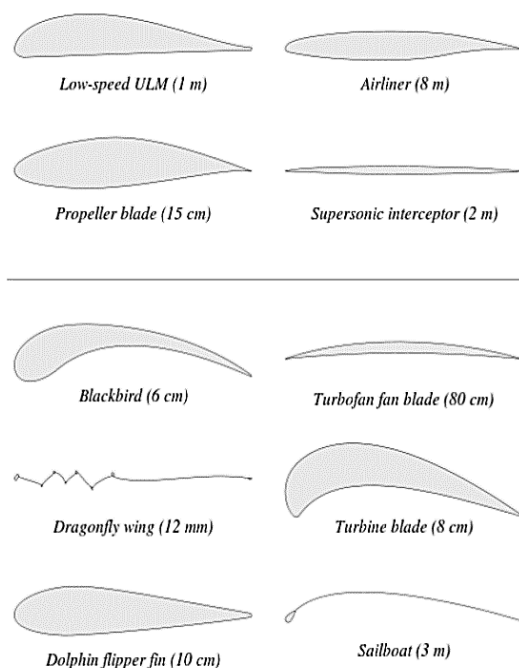

Figure 1. Airfoil types [15].

The aerodynamic performances are different due to the different geometry of the airfoil, and according to the behavior of different airfoil, choosing a workable blade for the wind turbine blade will improve the efficiency. To characterize an airfoil, Figure 2 was examined.
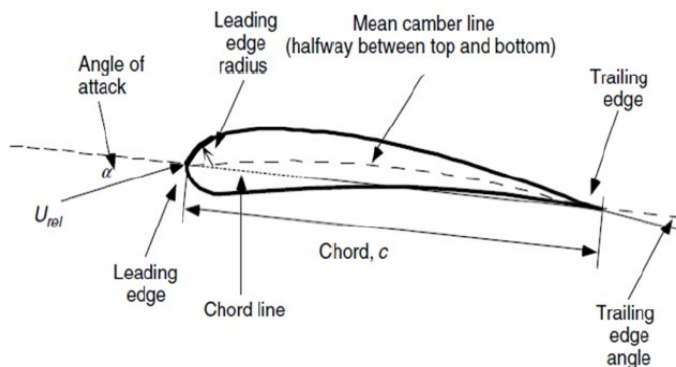

Figure 2. Parts of the airfoil [15].

Mean camber line: is the location of the points in the middle of the upper and lower surfaces of the airfoil. Leading edge: It is the most forward point of the airfoil. Trailing edge: It is the rearmost point of the airfoil. Chord line: connects the leading edge of the airfoil to the trailing edge. The chord line is a straight line and its distance is known as the chord "c" of the airfoil. Hump: is the distance between the chord line and the position representing the average hump line measured perpendicular to the chord line. Thickness: the thickness

of the airfoil at any point along the chord line is the distance between the top and bottom surface measured perpendicular to the chord line. Angle of attack (α): is the angle formed between the chord line and the relative wind direction.

Generally, there are two forces and a moment acting on the airfoil. These are lift, drag and moment as seen in Figure 3 [16].
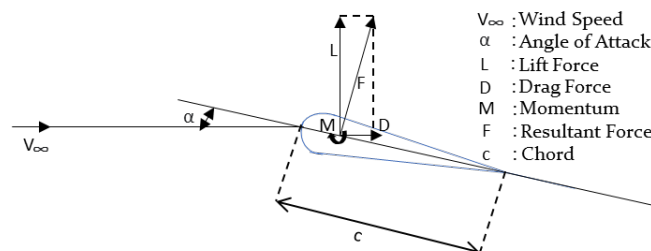

V_∞ : Wind Speed
α : Angle of Attack
L : Lift Force
D : Drag Force
M : Momentum
F : Resultant Force
c : Chord

Figure 3. Lift and drag ratio [16].

Lift is the force used to overcome gravity and is defined as perpendicular to the direction of the oncoming airflow. It occurs as a result of unequal pressure on the upper and lower wing surfaces. The higher the lift, the greater the mass that can be lifted off the ground. Drag force is defined as a force parallel to the direction of the incoming airflow. The drag force results from both viscous drag forces on the airfoil's surface and unequal pressure on the wing surfaces facing toward and away from the incoming flow. Lifting force;

$$F_L = C_L \, \tfrac{1}{2} \rho V^2 c \tag{1}$$

$$F_D = C_D \, \tfrac{1}{2} \rho V^2 c \tag{2}$$

$$M = C_M \, \tfrac{1}{2} \rho V^2 c \tag{3}$$

Here C_L is the lift coefficient, C_D is the drag coefficient and C_M is the moment coefficient. The C_L/C_D ratio is called the percolation ratio. It is desired that wind turbines and aircraft wings have a high glide ratio. The maximum glide ratio is generally between 5° and 10° angles of attack.
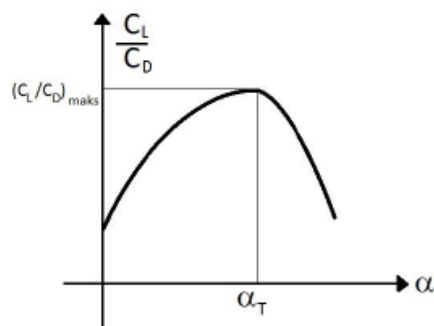

Figure 4. Design angle of attack graph [17].

The angle value (α_T) at which the glide ratio is highest in Figure 4 above is used as the design angle in the design of wind turbines [16]. Lift and drag coefficients vary with angle of attack. Polar graphs showing the change of these coefficient values with angle of attack are shown in Figure 5 [18].
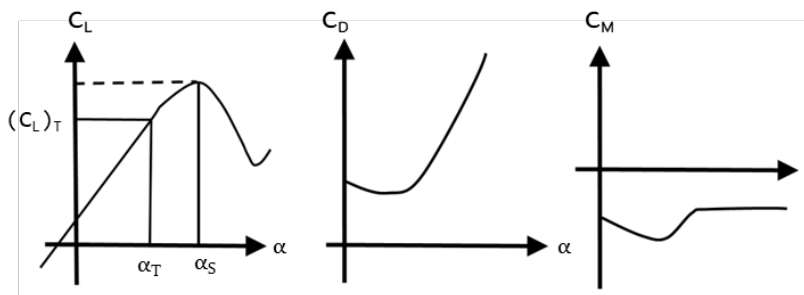
Figure 5. Polar graphics.

As the angle of attack increases, the lift and drag coefficient values also increase. This increase increases until a certain value of the angle of attack, and then the lift coefficient value begins to decrease. The drag coefficient value continues to increase rapidly. The flow moves in conformity with the surface at the top of the airfoil until the airfoil reaches this critical angle of attack. As the angle of attack increases, the flow begins to separate from the surface. As the flow separation approaches the leading edge of the airfoil, the lift coefficient value begins to decrease. This situation is called stall or loss of grip. This critical value of the angle of attack is called the stall angle [17].
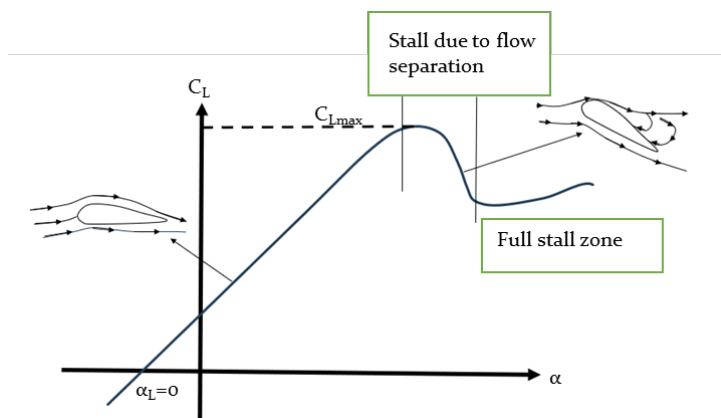

Figure 6. Flow separation occurring on the airfoil surface before and after stall [19].

Flow separation starts at the rear of the airfoil and shifts towards the front as the angle of attack increases (Figure 6). The flow separation and stall situation that occurs with increasing angle of attack are given in more detail in Figure 7. As the angle of attack increases, vortices form in areas where flow separation occurs. The drag coefficient also increases in these regions.
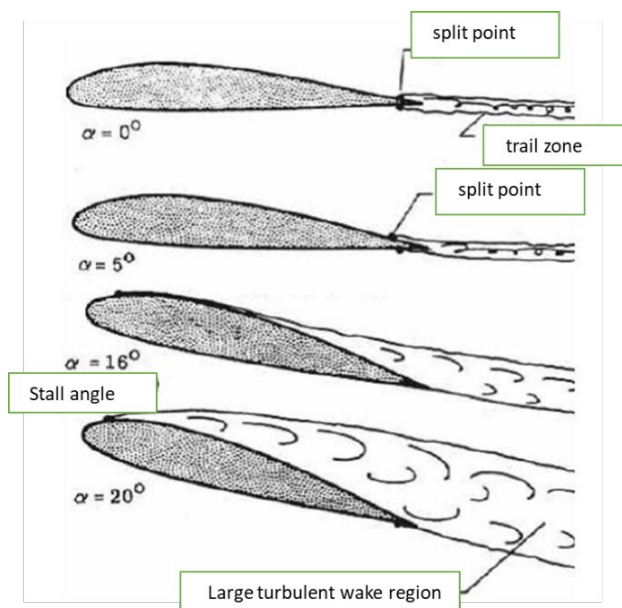
Figure 7. Flow separation and stall condition [19].

2.2. Two Dimensional Airfoil CFD Analysis

In the experimental investigation of the NACA 4412 airfoil, its length was 1 meter and its Reynolds number was approximately 6,000,000 [14]. In this study, the airfoil length was taken as 0.2 m. Therefore, a new analysis was needed because the Reynolds number and airfoil size would change. CFD analysis of NACA 4412 airfoil was performed using Ansys Fluent analysis program.

CFD is a good method used to improve many wind turbine blade designs and examine their aerodynamic performance [9], [20]. CFD analyzes have many advantages over experimental studies. The results of CFD analyzes can be examined in a short time with simulations. Additionally, results can be reproduced quickly. According to experimental results, the results of many parameters can be obtained simultaneously in CFD analysis. Additionally, values can be easily calculated in each cell element. In experimental studies, many prototypes need to be produced to improve the design, and this is a disadvantage in terms of both cost and time. In CFD analysis, design improvements can be made by examining simulations. This is advantageous both in terms of time and cost [21].

CFD is solved by Navier Stokes equations. Navier Stokes equations are momentum conservation and mass conservation equations and the results are obtained by solving them with the finite element method [22], [23]. The two-dimensional representation of these equations is as follows [24];

$$\frac{\partial u}{\partial x} + \frac{\partial v}{\partial y} = 0 \tag{4}$$

$$\rho u \frac{\partial u}{\partial x} + \rho v \frac{\partial u}{\partial y} = -\frac{\partial p}{\partial x} + \frac{\partial}{\partial y}\left[\mu(\frac{\partial v}{\partial x} + \frac{\partial u}{\partial y})\right] + \frac{\partial}{\partial x}(-\rho u'v') \tag{5}$$

$$\rho u \frac{\partial v}{\partial x} + \rho v \frac{\partial v}{\partial y} = -\frac{\partial p}{\partial y} + \frac{\partial}{\partial x}\left[\mu(\frac{\partial v}{\partial x} + \frac{\partial u}{\partial y})\right] + \frac{\partial}{\partial y}(-\rho u'v') \tag{6}$$

$$\tau_{xy} = -\rho u'v' = \eta(\frac{\partial u}{\partial y} + \frac{\partial v}{\partial x}) \tag{7}$$

The symbols u and v expressed in the above equations indicate the velocity com-ponents in the x and y directions. The letter P stands for pressure, the letter ρ stands for density, the letter μ stands for dynamic viscosity, and the letter τ stands for turbulent shear stress. The letters u' and v' indicate horizontal and vertical turbulence velocity deviations. The letter η seen in the turbulent shear stress equation represents turbulent viscosity. Three-dimensional versions of the Navier Stokes equations are also available. There are many turbulence

models developed for various situations. The most commonly used turbulence models are spalart allmaras, k-epsilon and k-omega. There is no turbulence model that covers all flows and gives the most accurate results. Therefore, the results obtained using different turbulence models for a flow can be examined and the one that gives the most logical result can be selected. In this study, the k-epsilon turbulence model was chosen [25].

Aerodynamic coefficient values (C_L, C_D, C_M) around an airfoil can be calculated experimentally, using theoretical formulas or using CFD [26], [27]. In this study, aerodynamic coefficients of airfoils were obtained using the CFD method. There are many stages when performing this method.

These stages are as follows: 2D coordinates of the determined airfoil were transfer-red to the computer program Ansys Fluent analysis program. A C-shaped flow field boundaries are created around the geometry of the airfoil as shown in Figure 8 below. This serves the purpose of the wind tunnel used in the experimental study. To create boundary conditions, velocity values were entered in the inlet section, which is the F curve. The pressure value is entered in the outlet section, which is line C. The G curve, which is the edge line of the airfoil, is specified as the wall-no-slip condition. Edges ED and AB are defined symmetrically [28].
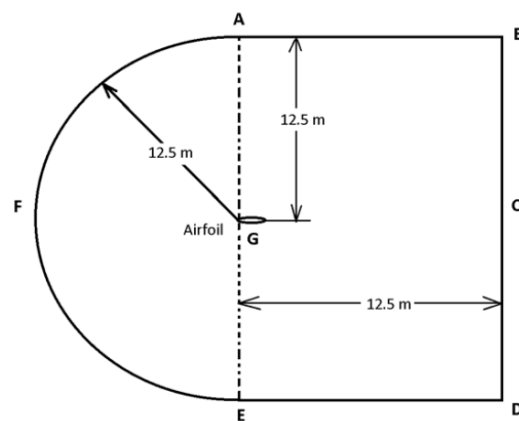

Figure 8. Airfoil flow field [29].

The resulting geometry and flow field are divided into cells in the mesh section. First, the unstructured triangular mesh was applied, and then the structured quadrangular mesh was applied (Figure 9). The purpose of dividing into small cells with mesh is to solve the conservation equations in each cell. One of the most important situations that increase the accuracy in computational fluid dynamics solution depends on these cells [28].
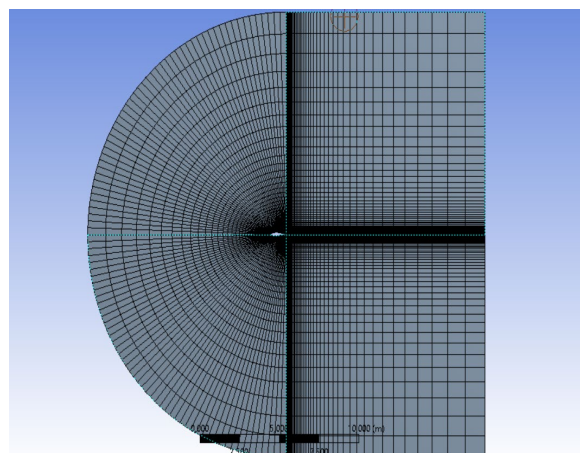

Figure 9. Structured mesh.

After creating the geometry, determining the necessary boundaries and meshing process were completed, the solution process of the Ansys program was started. Results were obtained from these analyzes performed at different angles of attack.

3. Results and Discussion

There are data for NACA 4412 airfoil in the literature. However, these data were obtained at different sizes of the airfoil and at high Reynolds numbers [30]. In this study, the airfoil size was determined as 0.2 meters. Therefore, a reanalysis was performed using the Ansys computer analysis program. While performing the analysis, the k-epsilon turbulence model was chosen as the turbulence model. Annual average wind data at some points received from the General Directorate of Meteorology were examined and it was decided to select the wind speed as 10 m/s. Analysis was carried out at each angle of at-tack of 0°, 2°, 5°, 8°, 10°, 12°, 15° and 18°. In the analyses, firstly the aerodynamic coefficients were obtained. Since these coefficient values are not reasonable values at angles of attack after 15 degrees, the analysis was carried out up to an angle of attack of 18 degrees. These values are graphed and shown in Figure 10.
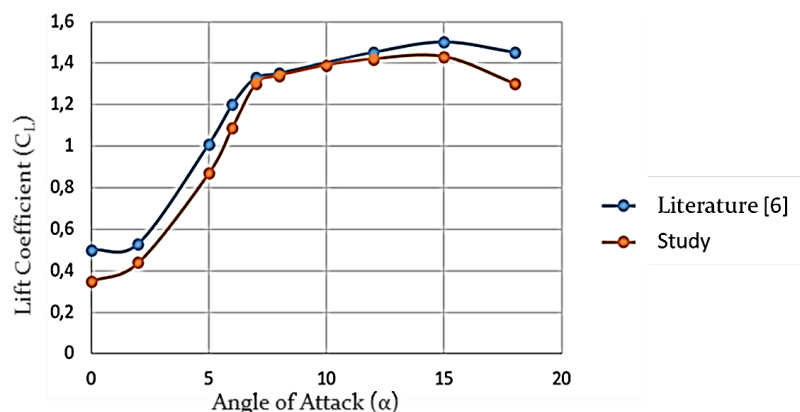

Figure 10. NACA 4412 lift coefficient.

The lift coefficient results from the analysis conducted for the NACA 4412 airfoil and the lift coefficient results obtained from the experimental study conducted in the literature [12] are given in Figure 10. Reynolds numbers vary because the airfoil size is de-signed to be 1 meter in the literature and 0.2 meters in this study. Therefore, there are deviations between the values given in Figure 10.
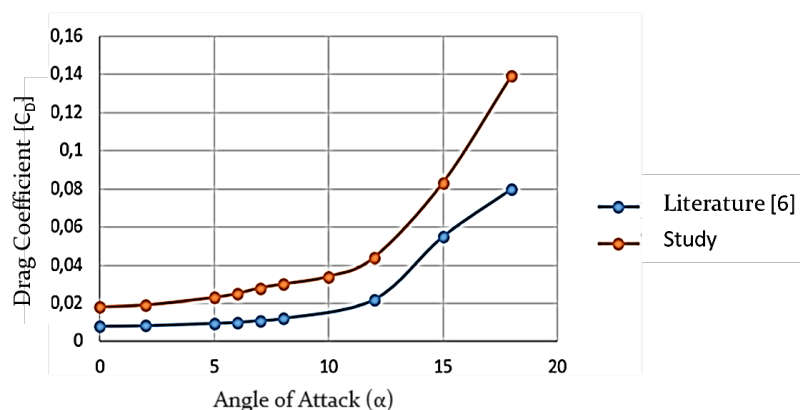

Figure 11. NACA 4412 drag coefficient.

The drag coefficient results from the analysis conducted for the NACA 4412 airfoil and the drag coefficient results obtained from the experimental study conducted in the literature [14] are given in Figure 11. There are deviations between the values due to the change of Reynolds number.
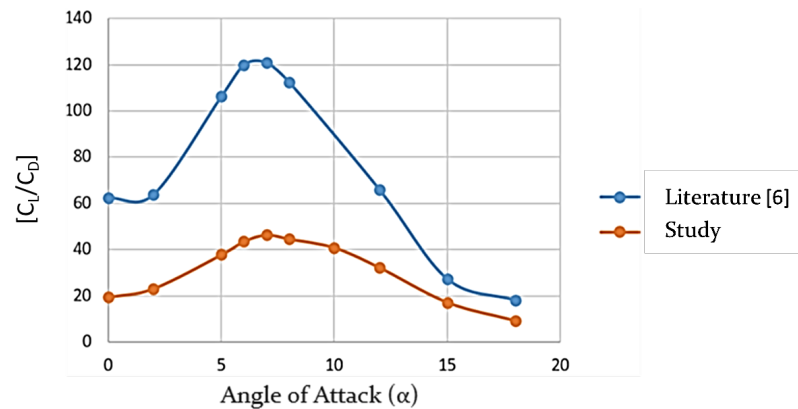
Figure 12. NACA 4412 glide ratio (C_L/C_D).

When we look at the percolation rate graph given in Figure 12, the values of the analysis performed in Ansys are lower. However, in both studies, the angle of attack with the highest glide ratio is 7 degrees. This shows that the analysis gives correct results. The reason for the difference in values between the two studies is that the wing length and Reynolds number are different. As stated in the studies for NACA 4412, the stall angle is 15 degrees. In this respect, examinations made with analysis programs do not yield logical results. Viterna equations were used to determine the aerodynamic coefficients at angles of attack up to 90 degrees. A polynomial function was created to determine the aerodynamic coefficient values before stall. In the analyzes performed in Ansys, a 4th degree function was defined using C_L and C_D values at angles of attack of 0°, 5°, 10°, 15°, 18°. The coefficients in the lift force polynomial and the coefficients in the drag force polynomial were found as in Table 1.

Table 1. NACA 4412 Aerodynamic coefficients before stall.

Lift force polynomial coefficients	C_L	Drag force polynomial coefficients	C_D
k0	0.35	t0	0.018
k1	0.03493	t1	0.003198
k2	0.02319	t2	–0.0007637
k3	–0.002122	t3	0.00006926
k4	0.00004942	t4	-0.8865×10^{-5}

Using these data, aerodynamic performance values at all angles of attack before the stall can be calculated. Viterna equations were used to determine the aerodynamic co-efficients at angles of attack after stall. The values obtained with these equations are given in Table 2.

Table 2. NACA 4412 post-stall aerodynamic coefficients.

A_1	1.455
A_2	0.3044
B_1	2.91
B_2	–0.1981
(C_L) stall	1.3
(C_D) stall	0.011

According to the coefficient values obtained, polar graphs showing the C_L and C_D values at post-stall angles of attack for the NACA 4412 airfoil were created as follows.
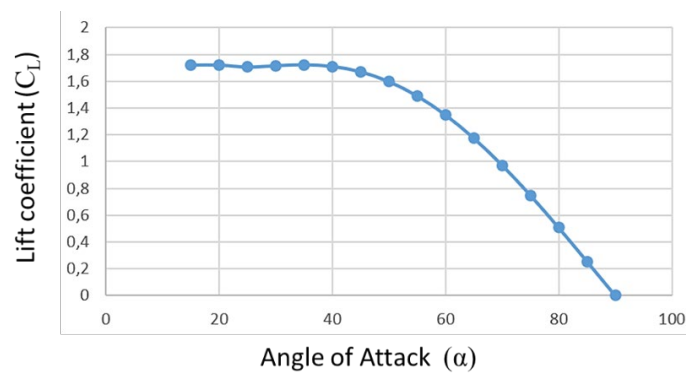
Figure 13. NACA 4412 post-stall lift coefficient values.

The lift coefficient values of the NACA 4412 airfoil in post-stall situations are shown graphically in Figure 13. When it reaches 90 degrees angle of attack, the lift coefficient becomes 0. Therefore, at a 90-degree angle of attack, no lift force will affect the airfoil.
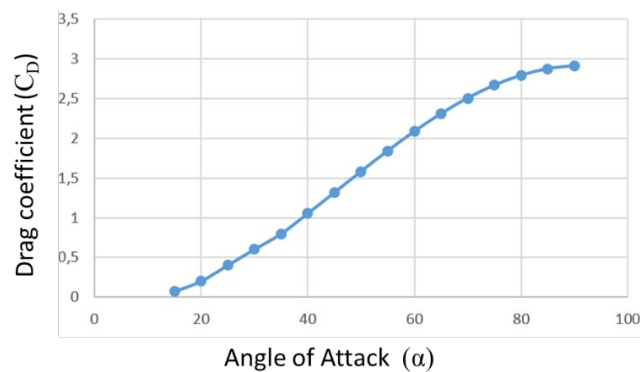

Figure 14. NACA 4412 post-stall drag coefficient values.

The drag coefficient values of the NACA 4412 airfoil in post-stall situations are shown graphically in Figure 14. In the stall condition, the drag coefficient took its lowest value. In this case, the aerodynamic performance of the airfoil is at its highest. When the angle of attack reaches 90 degrees, the drag coefficient reaches the highest value and the drag force acting on the airfoil reaches the highest value.

Lift and drag coefficient values at different angles of attack were found by two-dimensional CFD analysis of the NACA 4412 airfoil. Along with this analysis, the pressure and velocity contours affecting the airfoil were also examined. Each of the pressure and velocity contours at angles of attack of 0°, 2°, 5°, 8°, 10°, 12°, 15° and 18° are examined separately in Figure 15.
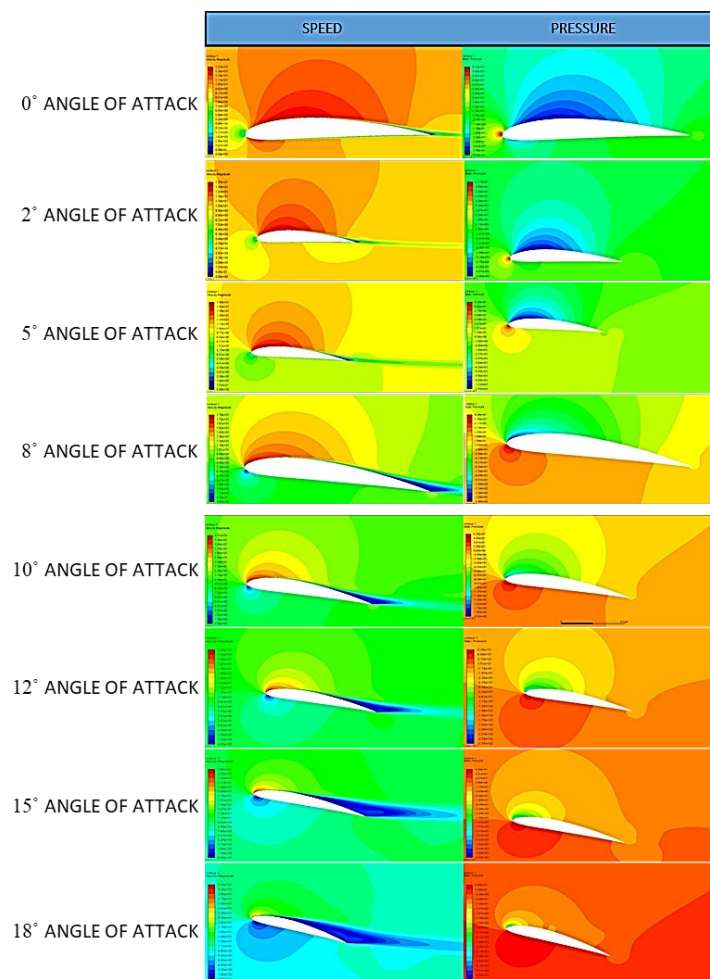
Figure 15. Speed and pressure values of NACA 4412 airfoil at different angles of attack.

The given pressure contours show that the pressure is high in the red, yellow and green regions, and that the pressure is low in the blue regions. The pressure at the leading ends of the airfoils is shown in red. Because the wind hitting this region is dampened, its speed becomes zero and the pressure becomes high [31].

When the pressure contours were examined as a whole, it was observed that the pressure values on the upper surface of the airfoil were lower than the pressure values on the lower surface [32].

When the speed contours are examined, it is understood that the wind speed is high in the red, yellow and green colored regions and low in the blue regions. The speed of the wind hitting the front parts of the airfoils becomes zero [31].

4. Conclusions

The aerodynamic properties of the NACA 4412 airfoil designed in the computer program were analyzed by the CFD method.

When the lift coefficient (C_L) and drag coefficient (C_D) values obtained both in experimental studies and in this study were compared with each other, small deviations occurred between the values. The reason for this is due to the differences in Reynolds numbers due to the change in airfoil length.

Angle of attack of 15 degrees is the stall angle of attack in both studies. In other words, after the angle of attack of 15 degrees, the lift coefficient value started to decrease.

Since the Reynolds number decreases as the angle of attack increases, the drag coefficient value increases. Increasing the drag coefficient value negatively affects aerodynamic performance.

When the pressure conditions affecting the airfoil are examined, as the angle of attack increases, the pressure difference between the front and rear parts of the airfoil increases. Under the influence of this pressure difference, the lifting force acts from the lower part of the airfoil to the upper part. According to this result, the higher the pressure at the bottom of the airfoil and the lower the pressure at the top, the higher the lift force.

When the speed situations are examined, as the angle of attack increases, the wind speed increases at the top of the airfoil and with the pressure generated at the bottom, the airfoil comes under the influence of the lifting force. After entering the stall state, the drag force will increase and the lift force will decrease. In this case, the airfoil cannot rise any further.

References

[1]. E. Kaya, K. ve Koç, "Yatay Eksenli Rüzgâr Türbinlerinde Kanat Profil Tasarımı ve Üretim Esasları," Mühendis ve Makina, vol. 56, no. 670, pp. 38–48, 2015.

[2]. A. Yılmaz, İ., Çam, Ö., Taştan, M., Karcı, "Farklı Rüzgar Türbin Kanat Profillerinin Aerodinamik Performansının Deneysel İncelenmesi," Politek. Derg., vol. 19, no. 4, pp. 577–584, 2016.

[3]. S. Güleren, K. M. ve Demir, "Rüzgar Türbinleri İçin Düşük Hücum Açılarında Farklı Kanat Profillerinin Performans Analizi," Isı Bilim. ve Tek. Derg., vol. 31, no. 2, pp. 51–59, 2011.

[4]. M. O. L. Hansen, "Chapter 2 2-D Aerodynamics", Aerodyn. Wind turbine Second Ed. Earthscan, UK USA, 2008.

[5]. M. Bakırcı, "Yatay eksenli rüzgar türbinlerinde optimum uç hız oranının incelenmesi," Doktora Tezi, Karabük Üniversitesi Fen Bilimleri Enstitüsü, 2018.

[6]. K. B. Navin, K. M. Paramasivam, M. Prasanna, and M. K. AZG, "Computational Fluid Dynamics Analysis of Aerodynamic Characteristics of NACA 4412 vs S809 Airfoil for Wind Turbine Applications," Int. J. Adv. Eng. Technol., vol. 7, pp. 168–173, 2016.

[7]. T. Kogaki, H. Matsumiya, K. Kieda, N. Yoshimizu, and Y. Yamamoto, "Performance Improvement Of Airfoils For Wind Turbines By The Modified Vortex Generator," in 2004 European Wind Energy Conference, 2004.

[8]. H. Suzuki, K. Rinoie, and A. Tezuka, "Laminar airfoil modification attaining optimum drag reduction by use of airfoil morp-hing," J. Aircr., vol. 47, no. 4, pp. 1126–1132, 2010.

[9]. D. Hartwanger and A. Horvat, "3D modelling of a wind turbine using CFD," in NAFEMS Conference, United Kingdom, 2008.

[10]. Sarada, S., Shivashankar, M., & Rudresh, " Numerical simulation of Viscous, incompressible flow around NACA 64618 subsonic airfoil using Computational Fluid Dynamics" Advances in Mechanical Engineering, 256, 2010.

[11]. Manga, P. J., Bello, A. A., Tijjani, M. A., Burari, F. W., AbdullAzeez, M. A., Teru, P. B., ... & Daniel, S. "Two-Dimensional Anal-yses Based Computational Fluid Dynamics On Naca 4412 Airfoil," Nigerian Journal of Sustainable Research, 1(1), 1-9, 2023.

[12]. Aminjan, K. K., Ghodrat, M., Heidari, M., Rahmanivahid, P., Khanachah, S. N., Chitt, M., & Escobedo-Diaz, J. P. "Numerical and experimental investigation to design a novel morphing airfoil for performance optimization," Propulsion and Power Re-search, 12(1), 83-103, 2023.

[13]. F. Bertagnolio, N. Sørensen, J. Johansen, and P. Fuglsang, "Wind turbine airfoil catalogue," Riso Natl. Lab. Roskilde, 2001.

[14]. A. E. Abbott, I.H. and Von Doenhoff, "Theory of wing sections, Including a summary of airfoil data," New York, USA: Dover Publications Inc. Copyright, 1959.

[15]. E. N. Prasad, S. Janakiram, T. Prabu, and S. Sivasubramaniam, "Design and Development of Horizontal Small Wind Turbine Blade for Low Wind Speeds," Int. J. Eng. Sci. Adv. Technol., vol. 4, no. 1, pp. 75–84, 2014.

[16]. M. O. L. Hansen, "Aerodynamics of Wind Turbines," Earthscan London, UK, 2008.

[17]. Anderson John D., "Fundementals of Aerodynamics," Third Edition. New York, USA: McGraw-Hill Book Company, 2001.

[18]. A. Yükselen, "Aerodinamik Ders Notları," İstanbul Teknik Üniversitesi, İstanbul, 2013.

[19]. Anderson John D., "Introduction to Flight," McGraw –Hill, 2000.

[20]. H. Cao, "Aerodynamics analysis of small horizontal axis wind turbine blades by using 2D and 3D CFD modelling," University of Central Lancashire, England, 2011.

[21]. L. N. Sezer, U. N., Guptab, A. and Longa, "Lecture Notes in Computational Science and Engineering," p. 67:457, 2009.

[22]. S. Sorensen, N. N., Michelsen, J. A. and Schreck, "Navier-Stokes predictions of the NREL phase VI rotor in the NASA Ames 80 ft x 120 ft wind tunnel," Wind Energy an Int. J. Prog. Appl. Wind Power Convers. Technol., vol. 5, no. 2–3, pp. 151–169, 2002.

[23]. E. Çengel, Y., Cimbala, Y. J. and Tahsin, "Akışkanlar Mekaniği Temelleri ve Uygulamaları," İzmir: Güven Kitapevi, 2008.

[24]. J. Anderson, John D. and Wendt, "Computational fluid dynamics," Springer, vol. 206, 1995.

[25]. M. Bakırcı, "Rüzgar Türbin Kanat Profil Optimizasyonu," Kırıkkale Üniversitesi, Fen Bilimleri Enstitüsü, Kırıkkale, 2014.

[26]. T. E. Bazilevs, Y., Hsu, M. C., Akkerman, I., Wright, S., Takizawa, K., Henicke, B., Spielman, T. and Tezduyar, "3D simulation of wind turbine rotors at full scale. Part I: Geometry modeling and aerodynamics," Int. J. Numer. methods fluids, vol. 65, no. 1–3, pp. 207–235, 2011.

[27]. D. A. Spera, "Wind turbine technology," Am. Soc. Mech. Eng. New York, USA, 1994.

[28]. Cornell University, "FLUENT Learning Modules," 2020.

[29]. R. D. Mahawadiwar, H. V., Dhopte, V.D., Thakare, P.S. and Ashedkar, "CFD analysis of wind turbine blade," Int. J. Eng. Res. Appl., pp. 3188–3194, 2012.

[30]. Hossain, S., Raiyan, M. F., Akanda, M. N. U., & Jony, N. H "A comparative flow analysis of NACA 6409 and NACA 4412 aerofoil," International Journal of Research in Engineering and Technology, 3(10), 342-350, 2014.

[31]. Yilmaz, M., Köten, H., Çetinkaya, E., & Coşar, Z. "A comparative CFD analysis of NACA0012 and NACA4412 airfoils," Journal of Energy Systems, 2(4), 145-159, 2018.

[32]. Qu, Q., Jia, X., Wang, W., Liu, P., & Agarwal, R. K. "Numerical study of the aerodynamics of a NACA 4412 airfoil in dynamic ground effect," Aerospace Science and Technology, 38, 56-63, 2014.